

5-1-1993

Adjustable levels of strong turbulence in a positive/negative ion plasma

D. P. Sheehan

University of San Diego, dsheehan@sandiego.edu

R. McWilliams

University of California, Irvine

N. Rynn

University of California, Irvine

Follow this and additional works at: <http://digital.sandiego.edu/phys-faculty>



Part of the [Physics Commons](#)

Digital USD Citation

Sheehan, D. P.; McWilliams, R.; and Rynn, N., "Adjustable levels of strong turbulence in a positive/negative ion plasma" (1993).

Physics and Biophysics: Faculty Publications. 1.

<http://digital.sandiego.edu/phys-faculty/1>

This Article is brought to you for free and open access by the Department of Physics and Biophysics at Digital USD. It has been accepted for inclusion in Physics and Biophysics: Faculty Publications by an authorized administrator of Digital USD. For more information, please contact digital@sandiego.edu.

Adjustable levels of strong turbulence in a positive/negative ion plasma

D. P. Sheehan^{a)}

Department of Physics, University of San Diego, San Diego, California 92110

R. McWilliams and N. Rynn

Department of Physics, University of California, Irvine, California 92717

(Received 5 October 1992; accepted 19 January 1993)

Positive/negative ion plasmas, composed of Ba^+ , SF_6^- , and residual electrons, were observed to display characteristics of strong turbulence. Experiments on the UCI Q machine linked the presence of negative ions (and the depletion of electrons) with large density fluctuations ($\delta n/n \approx 1$), large-amplitude, low-frequency electrostatic noise ($f \leq 20$ kHz), and rapid transport of ions across magnetic field lines ($D_{\perp} \approx 10^4$ cm²/sec). Ion velocity distributions were heated parallel to and cooled perpendicular to the confining magnetic field. The partial pressure of gaseous SF_6 was shown to serve as a regulator of plasma turbulence. Turbulence levels could be smoothly varied from quiescent states ($\delta n/n \approx 0.01$) to strongly turbulent states ($\delta n/n \approx 1$).

I. INTRODUCTION

Positive-negative ion plasmas (PNIP) are charge-neutral plasmas in which the negative charge is dominated by negative ions rather than electrons. PNIP's are interesting both experimentally and theoretically. They are found in gas laser discharges, combustion products,¹ plasma discharges for semiconductor device manufacture,² stellar atmospheres,³ pulsar magnetospheres,⁴ the Earth's ionosphere,^{5,6} and neutral beam sources for controlled fusion experiments.⁷ In recent years, PNIP's have been created artificially in the ionosphere by rocket releases of electron scavengers such as CF_3Br , $Ni(CO)_4$, and SF_6 , Ref. 8. These PNIP's display characteristics of strong turbulence.

From theoretical and experimental standpoints, PNIP's can be simpler to understand and diagnose than electron-ion plasmas because (1) many basic plasma processes are expected to be slowed in PNIP's relative to electron-ion plasmas due to the large mass of negative ions compared with electrons; (2) if electrons were to be entirely absent, the approximate mass symmetry between positive and negative species simplifies many analytical expressions, particularly wave dispersion relations; (3) by symmetry, diagnosis of one species can allow inferences about the other; and (4) sophisticated spectroscopic diagnostics can be applied to ions which cannot be applied to electrons. Also, there is good reason to believe that PNIP's should display features of strong turbulence, and, therefore, could serve as a simple experimental model to test strong turbulence theory.⁹⁻¹³ Plasma turbulence is important to plasma heating, mixing, and transport. Its deleterious effect on particle confinement in controlled fusion experiments is considered one of the chief impediments to useful nuclear power.¹⁴ PNIP's have been studied by a number of investigators over the last 30 years.¹⁵⁻²⁴

This paper will discuss evidence of strong turbulence found in a laboratory PNIP, specifically, large density fluctuations, rapid ion transport across magnetic field lines, broadband (turbulent) waves, and heating of the plasma

ions by the turbulence. The magnitude of this turbulence can be simply determined by setting a single experimental parameter: the vessel partial pressure of an electron-scavenging gas, SF_6 . We are aware of no other plasma system whose turbulence level can be varied so simply between such marked extremes—from quiescent to strongly turbulent. As such, this plasma may serve as a testing ground for models of strong turbulence.

This paper will be organized as follows: Sec. I A will present a brief overview of criterion for strong turbulence; Sec. II will describe experimental techniques; Sec. III results; and Sec. IV discussion of results.

A. Criterion for strong turbulence

Plasma turbulence may be defined in a number of ways. Among these, we will use a commonly cited parameter,^{9,11} $W \equiv \beta/\alpha$, the ratio of wave energy density, β , to particle kinetic energy density, α . Quasilinear or weak turbulence theory may be appropriate for the conditions $W \ll 1$. Intuitively, this indicates that wave amplitudes are too small to trap the majority of particles or to severely distort particle velocity distributions. The condition $W > 1$ can signal strong turbulence. Here, wave energy and particle kinetic energy densities are comparable such that the waves strongly influence the evolution of plasma properties. The W ratio may be restated in terms of wave potential and plasma density fluctuations. Via the Boltzmann relation, $\delta n/n \approx \exp(e\delta\phi/kT)$, with $\delta\phi$ representing the wave amplitude, one sees that $\delta n/n > 1$ is roughly equivalent to $W > 1$. Also, W may be estimated from changes in particle kinetic energy density as wave and particle energies equilibrate.

II. EXPERIMENT

Experiments were carried out in the UCI Q machine^{25,26} in a 5 cm diam, 1.3 m long Ba^+/e^- plasma column confined by a 1–7 kG solenoidal magnetic field. The vessel's base pressure is 1×10^{-6} Torr. The initial Ba^+/e^- plasma is produced by contact ionization of an atomic beam of Ba impinging on a rhenium-coated tung-

^{a)}Work performed at University of California, Irvine, California 92717.

sten disk (5 cm diam) heated to over 2000 K by electron bombardment. Electrons, thermionically emitted from the hot plate, accelerate charge-neutralizing Ba ions off the plate to a drift velocity of $1-2 \times 10^5$ cm/sec. The ion drift time down the vessel is roughly 1 msec. The electron and ion temperatures are initially those of the hot plate, about 0.2 eV. Typical plasma densities are 10^8-10^{10} cm $^{-3}$. In the following discussion, "parallel" and "perpendicular" will refer to the directions parallel or perpendicular to the solenoidal magnetic field. "Axial" and "radial" will refer also to the parallel and perpendicular directions.

Positive-negative ion plasmas are created from the Q-machine plasma by introducing gaseous SF $_6$ into the vacuum chamber. Sulfur hexafluoride is an electron scavenger with particular affinity for electrons with energies less than about 0.2 eV (≈ 2000 K).²⁷ By increasing the concentration of SF $_6$, the electron density in the plasma column can be reduced down to less than 0.01 of its initial value. The mass ratio of SF $_6$ to Ba, $m_{\text{SF}_6}/m_{\text{Ba}} = 146/137 = 1.07$, is very close to unity. A more detailed discussion of this and other PNIP sources is found in Sheehan and Rynn.²⁸

For this experiment, wave amplitudes were diagnosed by small wire antennae (tip length 2 mm), plasma densities by Langmuir probes (tip diameter 0.6 mm), and barium ion densities and velocity distributions by a laser-induced fluorescence (LIF) diagnostic which has been discussed in detail elsewhere.^{29,30} The spatial, velocity, and temporal resolutions of this diagnostic are roughly 1 mm,³ 30 m/sec, and 10^{-9} sec, respectively.

Doppler broadened Ba(II) velocity distributions are resolved by virtue of the narrow frequency bandwidths of the tunable dye laser ($\Delta\nu \sim 2$ MHz) and the natural linewidth of the Ba(II) atomic transitions ($\Delta\nu \sim 21$ MHz) and the relatively broad effective frequency bandwidth of the ion thermal velocity distribution ($\Delta\nu \sim 2$ GHz). An individual ion may undergo a laser-induced atomic transition when the laser photon, (ω_L, \mathbf{k}_L) , the ion velocity, \mathbf{v}_i , and the atomic transition angular frequency, ω^* , satisfy the Doppler relation

$$\omega^* = \omega_L - \mathbf{k}_L \cdot \mathbf{v}_i. \quad (1)$$

As the dye laser is swept in frequency, the strength of the fluorescence signal is proportional to the ion density in the narrow velocity interval \mathbf{v} to $\mathbf{v} + \Delta\mathbf{v}$ satisfying Eq. (1) and the natural linewidth of Ba(II). From the resultant fluorescence signal strength versus frequency curve, the one dimension ion velocity distribution is generated. A schematic of the experimental setup is presented in Fig. 1. The laser can be aligned perpendicular or parallel to the magnetic field to obtain perpendicular or parallel Ba(II) velocity distributions. Temperatures were assigned to non-Maxwellian distributions based on their best fits to Maxwellians.

III. RESULTS

Positive-negative ion plasmas in the Q machine displayed evidence of strong turbulence, namely large density

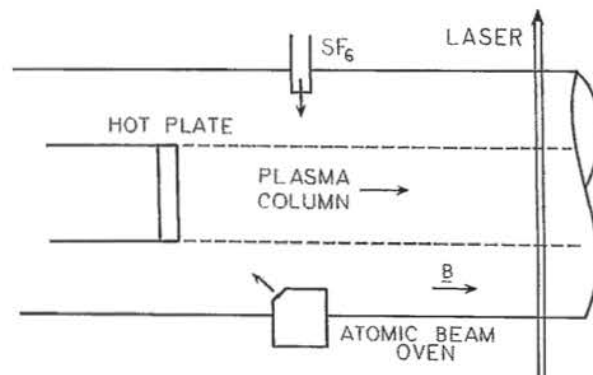


FIG. 1. Schematic of Q machine and LIF diagnostic configured to measure ion perpendicular velocity distribution.

fluctuations, strong low-frequency electrostatic turbulence, rapid crossfield diffusion, and ion heating. Some initial results are found in Sheehan and Rynn.²⁸

Density fluctuations ($\delta n/n \geq 1$) measurements were made using Langmuir probes. For a fixed plasma density, increased density fluctuations were obtained by increased SF $_6$ concentrations. In Fig. 2, ion density fluctuation levels, $\delta n/n$, are presented versus partial pressure SF $_6$ for a plasma of initial density 4×10^9 cm $^{-3}$ and magnetic field $B = 3$ kG. Here δn is the value of the density fluctuations and n the average ion density. The density fluctuation level, δn , was taken to be roughly 90% of the maximum value of ion density spikes observed in Langmuir probe current-voltage ($I-V$) traces. An exemplary $I-V$ trace is found in Fig. 4 of Sheehan and Rynn.²⁸ Note that values of $\delta n/n$ in excess of unity are not forbidden for many nonsinusoidal signals.

Data in Fig. 2 in this present paper were taken at the center of the plasma column. Before SF $_6$ was introduced, the plasma was quiescent with $\delta n/n \approx 0.01$. At $P_{\text{SF}_6} = 2 \times 10^{-5}$ Torr, the residual electron density was roughly 0.03 of its pre-SF $_6$ value ($n_e/n_{e0} \approx 0.03$) and the density fluctuations had increased to roughly 25 times their

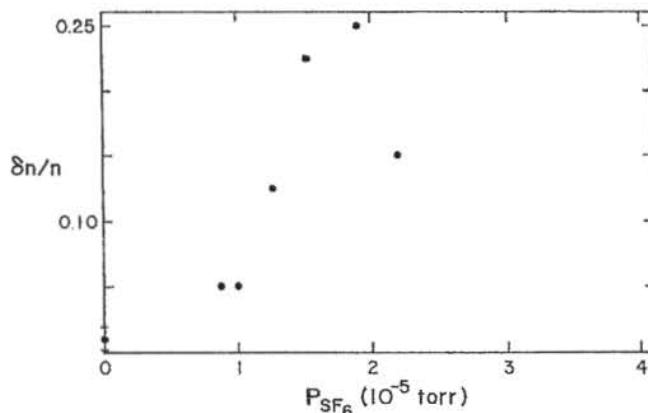


FIG. 2. Plasma density fluctuation level, $\delta n/n$, versus partial pressure SF $_6$.

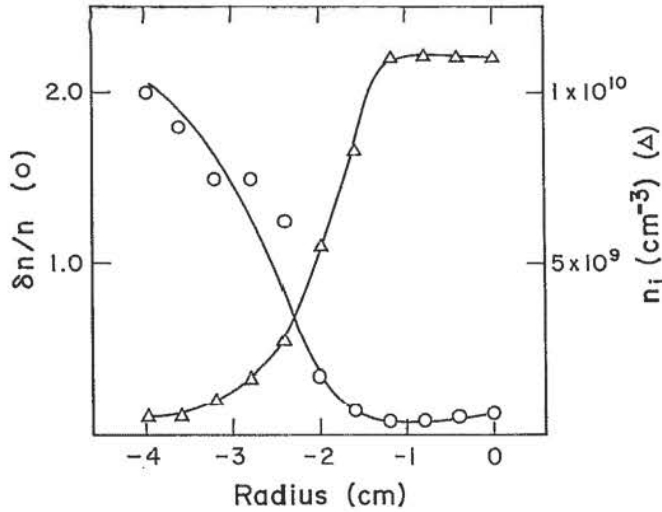


FIG. 3. Fluctuation level, $\delta n/n$, and plasma density versus plasma radius. Plasma parameters: $B=3$ kG, $r=0$ cm.

initial value, $\delta n/n \approx 0.25$. The rolloff in $\delta n/n$, seen at the highest pressure, is probably due to large radial losses of energetic plasma particles. At these pressures, the plasma has probably changed beyond the range of meaningful comparison to other data points.

Density fluctuation levels varied across the plasma column diameter, as shown in Fig. 3. Here $r=0$ cm is the center of the plasma column and $r=-2.5$ cm corresponds to the edge of the plasma column before SF_6 was introduced. Notice that for $r < -2.0$ cm, $\delta n/n$ increases sharply up to a value of $\delta n/n \approx 2$. The region $r < -2.0$ cm should be especially depleted in electrons since few electrons are expected to undergo the multiple scatterings necessary to reach these radii. At 3 kG, a 0.2 eV electron gyroradius is minute, ($\rho_e \sim 3 \times 10^{-4}$ cm). For $r < -2.5$ cm, residual electron densities were below the detection limit of Langmuir probes ($n_e/n_{e0} < 10^{-4}$).

At low plasma densities and high partial pressures of SF_6 , positive and negative ions are observed to undergo very rapid transport across magnetic field lines. Normally, a Q machine plasma is a tightly confined column; its diameter might increase only a few percent from its origin to termination. However, as the electron density is depleted, the plasma column expands rapidly in the radial direction (perpendicular to B) as the plasma flows axially away from the source. Based on measured plasma drift velocities and on radial ion density profiles downstream from the hot plate, one can infer cross-field diffusion coefficients in excess of 10^4 cm²/sec for PNIP's with low-electron densities. These large values of D_1 are in reasonable agreement with Dupree^{31,32} and McWilliams³³ scaling laws for cross-field transport. Dupree and McWilliams scalings can be written in the general form $D_1 = \gamma(cT/eB)(\delta n/n)$ where c is the speed of light, T is temperature, e is species charge, B is magnetic field, and γ is a proportionality constant; for Dupree $\gamma = 1/\sqrt{2}$ and for McWilliams $\gamma = 3.7$. For our experimental conditions ($B=3$ kG, $T=0.2$ eV, $\delta n/n \approx 2$) Du-

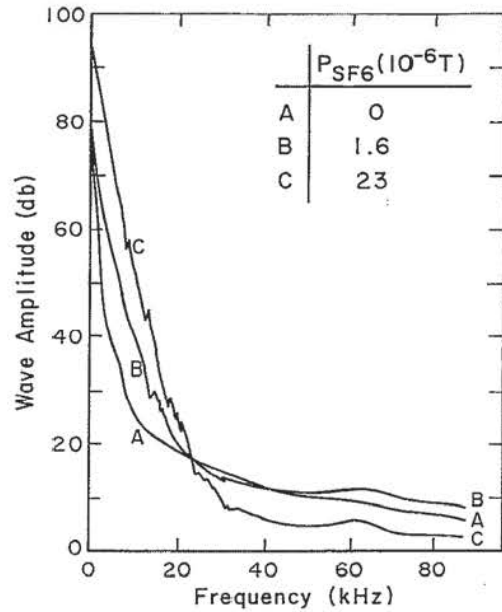


FIG. 4. Turbulent wave intensity versus frequency for three partial pressures SF_6 . Plasma parameters: $n=8 \times 10^9$ cm⁻³, $B=3.5$ kG.

pre scaling predicts $D_1 \sim 2 \times 10^3$ cm²/sec and McWilliams predicts $D_1 \sim 10^4$ cm²/sec.

Low-frequency electrostatic noise ($f < 20$ kHz) was observed in all regions of PNIP's and was found to dominate the wave spectra of all PNIP's studied here. Its intensity was found to increase roughly in proportion to $\delta n/n$, and it saturated in magnitude within about 20 cm of the hot plate. (Port access precluded measurements of the plasma nearer than 20 cm.) In Fig. 4 examples of wave spectra are presented for three representative partial pressures of SF_6 . Higher-frequency turbulence was sought up to about ten times the ion plasma frequency $f \sim 10\omega_{pi} \approx 20$ MHz, but none was observed. The frequency range of the noise in Fig. 4 is appropriate for the electrostatic drift wave, Kelvin-Helmholtz wave, the potential relaxation instability, and current-driven ion acoustic wave. The latter two have been studied in PNIP's at the University of Iowa.^{34,35} Neither of these were identified in the present experiments. The broadband wave spectrum that overlaps the Iowa results, and which we report here, has not yet been identified as any particular wave or instability. Due to its turbulent nature, conclusive identification of it may be a formidable task. A bibliography of waves found in Q machines can be found in Ref. 36.

Ba(II) parallel and perpendicular velocity distributions, obtained by LIF techniques, were altered substantially when SF_6 was introduced. Examples of ion velocity distributions with and without SF_6 are shown in Fig. 5. Given its strong parallel and perpendicular interactions with ion velocity distributions, one might speculate that the turbulence's parallel and perpendicular phase velocities are comparable to ion thermal and drift velocities. Perpendicular velocity distributions cooled and lost particles with increased SF_6 pressure. This may be explained by prefer-

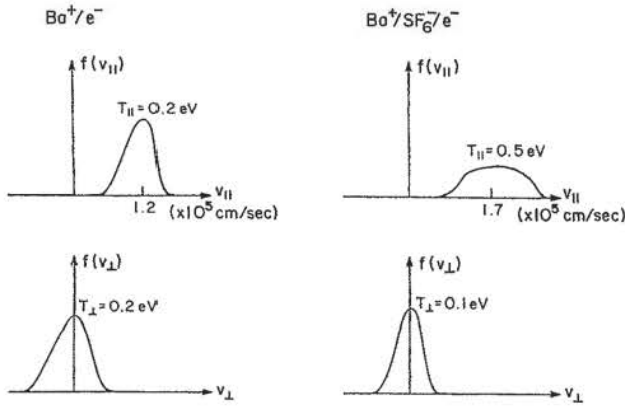


FIG. 5. Typical parallel and perpendicular Ba(II) velocity distributions for Ba^+ / e^- and $\text{Ba}^+ / \text{SF}_6^- / e^-$ plasmas. Plasma parameters: $n = 2 \times 10^9 \text{ cm}^{-3}$, $P_{\text{SF}_6} = 1 \times 10^{-5} \text{ Torr}$, $B = 3 \text{ kG}$.

ential radial diffusion of high v_{\perp} ions compared to low v_{\perp} ions as the plasma transited the vacuum vessel. Observations of rapid radial expansion and density depletion of the plasma column support this explanation.

Parallel velocity distributions exhibited complex alterations with the introduction of SF_6 . Parallel distributions lost ions, but in a non-Maxwellian manner and, in addition, they heated and appeared to increase their drift velocities. Figure 6 plots parallel ion temperatures versus partial pressure SF_6 and Fig. 7 plots the distributions apparent drift velocity versus SF_6 partial pressure. The increased drift velocity may be an artifact of preferential loss of low v_{\parallel} particles. If this is the case, then the parallel heating is actually more dramatic than shown in Fig. 6. Before SF_6 was introduced, the Ba^+ / e^- plasma's parallel and perpendicular temperatures are roughly that of the hot plate, about 0.2 eV.

IV. DISCUSSION

The results of the last section can be explained by the action of strong turbulence on the ions. First, the large

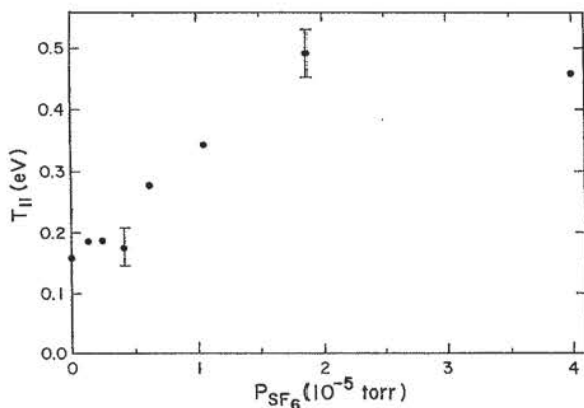


FIG. 6. Ba(II) parallel temperature versus SF_6 partial pressure. Plasma parameters: $n = 2 \times 10^9 \text{ cm}^{-3}$, $B = 3 \text{ kG}$.

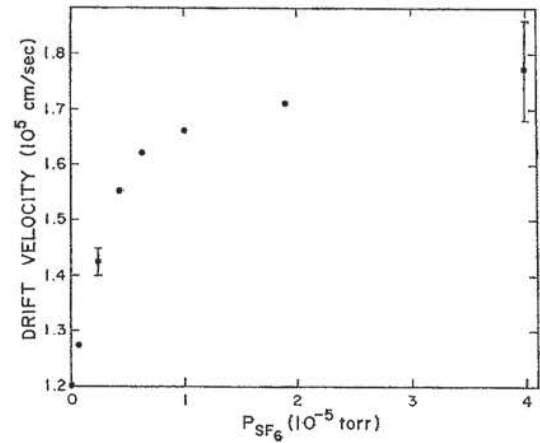


FIG. 7. Apparent Ba(II) parallel drift velocity versus SF_6 partial pressure. Plasma parameters: $n = 2 \times 10^9 \text{ cm}^{-3}$, $B = 3 \text{ kG}$, $z = 80 \text{ cm}$ from hot plate.

density fluctuations observed in the PNIP's are expected given large amplitude waves. This is suggested by the Boltzmann relation. If, for example, wave potentials were on the order of 0.2 V, which are sufficiently large to draw in and expel a large fraction of the 0.2 eV ion population from a given region of space, the Boltzmann relation predicts $\delta n/n \approx 1$, which was observed experimentally.

Modifications to the ion velocity distributions can be explained by turbulent wave-particle interactions. Recall that ion parallel velocity distributions heat and appear to increase their drift velocities with increased partial pressure of SF_6 (see Figs. 6 and 7). Several observations support strong turbulence heating. First, wave potentials, as indicated by density fluctuations and wave spectra, are probably large enough to trap and heat ions. Second, the entire velocity distribution appears heated as would be the case for broadband noise and a wide variation in wave-phase velocities. This is in contrast to what would be expected for a coherent wave or instability³⁷ which would tend to modify that part of the distribution that matches its phase velocity. Third, ion heating is very rapid, apparently occurring on a time scale of a few plasma fluctuation periods. The transit time for an ion from the hot plate to the detection region is roughly $\tau_{\text{transit}} \approx 5 \times 10^{-4} \text{ sec}$, whereas a typical fluctuation period for the turbulence is on the order of $\tau_{\text{turb}} \approx 2 \times 10^{-4} \text{ sec}$ at 5 kHz. This suggests that ions can be strongly heated (a factor of 2 increase in temperature) in just a few fluctuation periods.

The apparent increase in ion drift velocity, v_d , also is consistent with wave-particle interactions. One might attribute the increase in v_d to an increase in the hot plate sheath potential, but it is not evident why this should be. On the other hand, ion collisions can account for the salient results. Ions with smaller v_{\parallel} would take longer to reach a given z position away from the plasma source. Hence, smaller v_{\parallel} ions spend more collision times between the source and observation point. The smaller v_{\parallel} ions thus may be expected to be lost radially preferentially to fast ions. This would lead to the reduced ion densities and

increased ion drift speeds at the observation point in the plasma. This collision process also suggests $f(v_{\parallel})$ should develop a non-Maxwellian character, since ions of different v_{\parallel} have different probabilities of reaching the detection region. This, too, is observed experimentally. Note that, if a substantial fraction of the lower v_{\parallel} ions were lost from the plasma column, the parallel heating indicated in Fig. 6 probably underestimates the true heating that occurred. Based on the apparent increase in drift velocity of $f(v_{\parallel})$, the actual plasma temperature may have been in excess of 1 eV before being lost to the walls. This suggests that the ions may have been heated a factor of 5 or more in temperature in just a few fluctuation periods!

The cooling of the perpendicular distribution can be explained also by wave-particle heating. Let us assume that the turbulence heats $f(v_{\perp})$, but that the component waves have phase velocities high enough such that they interact preferentially with high v_{\perp} ions. These high v_{\perp} ions, by virtue of their larger Larmor radii, leave the plasma column radially preferentially to low v_{\perp} ions and are lost to the chamber walls. The distribution, now poor in high v_{\perp} ions, appears cooled.

Particle-particle collisions do not adequately explain the bulk of these results. Although they may contribute partially to the large values of cross-field particle diffusion, they cannot explain the large density fluctuations, the substantial parallel heating, perpendicular cooling, or drift velocity changes of the ion velocity distribution.

Let us summarize the probable evolution of the plasma from origin to termination. A Ba^+/e^- plasma is created at the hotplate at a temperature of 0.2 eV and begins to drift down the vessel with an initial drift velocity $v_d = 1.2 \times 10^5$ cm/sec. Electrons are scavenged by SF_6 gas and a broadband, low-frequency, strong turbulence insues and saturates within 20 cm of the hotplate, driving large plasma density fluctuations. The turbulence possibly possesses a broadband parallel and perpendicular wavelength spectrum which allows it to heat both components of the ion velocity distribution. The perpendicular velocity distribution is initially heated and, through preferential loss of high v_{\perp} ions, cools. Meanwhile, the parallel distribution, which remains in the presence of the turbulence during its vessel transit, heats and preferentially loses low v_{\parallel} ions to the walls and, thereby, apparently increases its drift velocity and develops a non-Maxwellian character.

A. Estimate of the W ratio

Much of the experimental data thus far presented suggest that PNIP's are strongly turbulent systems. We will use $W \gg 1$ as a working criterion for strong turbulence. The roughly equivalent statement, $(\delta n/n) \gg 1$, has been met ostensibly (Fig. 3). We will attempt to demonstrate $W \gg 1$ from other experimental data. The W ratio can be calculated from separate calculations of wave and particle kinetic energy densities. Particle kinetic energy densities require detailed knowledge of $f(v_{\parallel})$ and $f(v_{\perp})$. Both are available, but are incomplete due to radial losses. One can, however, make lower limit estimates of ion kinetic energy densities by using the depleted distributions. The parallel

distribution seems to be more representative of the heating undergone by the ions than does the perpendicular distribution, therefore, the former will be used. The kinetic energy density for the parallel distribution, α_{\parallel} , is defined as

$$\alpha_{\parallel} = \frac{1}{2} mn \int_{-\infty}^{\infty} v_{\parallel}^2 f(v_{\parallel}) dv_{\parallel} . \quad (2)$$

Here m is the ion mass and n is the ion number density. We will take α_{\parallel} to be representative of the total ion kinetic energy density, α . As a rough estimate for calculation of W , we will take α to be the ion kinetic energy density before SF_6 is added, that is, $\alpha = \alpha_{\text{initial}}$.

Wave energy density, β , for electrostatic waves is defined as

$$\beta = \frac{1}{8\pi} \int_{-\infty}^{\infty} |E_k|^2 dk, \quad (3)$$

where E_k is the k -space electric field component. Experimentally, direct and accurate measurement of E_k is difficult and its indirect measurement based on wave dispersion relations, potential and density fluctuations levels involve several uncertainties. The application of Eq. (3) to the present PNIP is questionable. Not only has the wave or instability responsible for the broadband turbulence not been conclusively identified, but its large-amplitude, broadband nature would make any dispersion relation suspect. Calculations of E_k from the spectral floating potential, Φ_k , requires the spectral density fluctuation, δn_k , which could not be obtained.

For this calculation, rather than use Eq. (3), we will use experimental values of ion heating to estimate β . It is reasonable to assume that the ion heating is entirely the result of turbulence since particle-particle collisions cannot account for it. One may take as a reasonable lower limit of β the difference between the final and initial ion kinetic energy density, that is, $\beta \gg \alpha_{\text{final}} - \alpha_{\text{initial}}$; in fact, β may be considerably greater than this. Here α_{initial} is the ion kinetic energy density without SF_6 and α_{final} is its value with SF_6 . Now, one can estimate W as

$$W \equiv \frac{\beta}{\alpha} \approx \frac{\alpha_{\text{final}} - \alpha_{\text{initial}}}{\alpha_{\text{final}}} . \quad (4)$$

Experimental velocity distributions were numerically integrated to obtain α . A plot of W versus SF_6 partial pressure is shown in Fig. 8(a) for the pressure range $0-30 \times 10^{-6}$ Torr. W increases rapidly with SF_6 pressure up to roughly 0.5 for $P = 10^{-5}$ Torr, then rolls over, due in part to plasma density depletion. In calculating W , the estimate of β is probably low. First, β has been equated merely to the change in ion kinetic energy density when, actually, wave amplitudes remain large even after ions have been heated. This suggests that the wave fields store additional energy that was not deposited in ion thermal energy and, thus, that β in Eq. (4) may be a low estimate. Second, the radial loss of ions has not been compensated for in these calculations; that is, the kinetic energy of ions leaving the plasma is not counted in calculations of α_{final} . For reference, between $P_{\text{SF}_6} = 0$ Torr and $P_{\text{SF}_6} = 10^{-5}$ Torr, up to

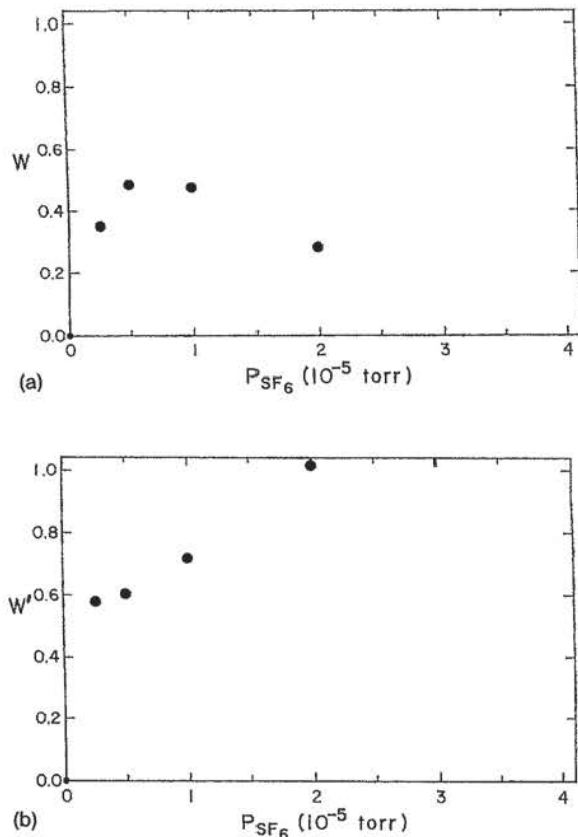


FIG. 8. Turbulence level versus SF_6 partial pressure. (a) Turbulence ratio, W , versus SF_6 partial pressure; (b) Alternative turbulence ratio, W' , versus SF_6 partial pressure. Plasma parameters: $n=2 \times 10^9 \text{ cm}^{-3}$, $B=3 \text{ kG}$, Pre- SF_6 W ratio, $W \approx 0.01$.

half the plasma may be lost radially. This may account largely for the rolloff in W at higher SF_6 pressures. An alternative way to calculate W is to normalize α_{final} in order to compensate roughly for radially lost ions. This can be done by multiplying α_{final} by the normalizing factor $n_{\text{initial}}/n_{\text{final}}$. In doing so, one obtains a new W ratio we call W' . A plot of W' versus partial pressure SF_6 is given in Fig. 8(b).

Figure 8 indicates the turbulence level in the PNIP can be varied smoothly by varying SF_6 partial pressure from a quiescent state characteristic of the Q-machine plasma up to a strongly turbulent state.

ACKNOWLEDGMENTS

The authors would like to thank Mr. D. Parsons and Mr. S. Keller for valuable laboratory assistance.

This work was sponsored by National Science Foundation Grant No. PHY-9024667, a University of San Diego Faculty Research Grant (1992), and by a Cottrell College Science Award of Research Corporation.

- ¹V. G. Dresvyannikov and O. I. Fison, *Teplofiz. Vys. Temp.* **14**, 1275 (1976).
- ²R. A. Gottscho, G. P. Davis, and R. H. Burton, *Plasma Chem. Plasma Proc.* **3**, 193 (1983).
- ³H. Massey, *Negative Ions*, 3rd Ed. (Cambridge University Press, Cambridge, 1976).
- ⁴M. A. Ruderman and P. G. Sutherland, *Astrophys. J.* **196**, 51 (1975).
- ⁵J. M. Kindel and C. F. Kennel, *J. Geophys. Res.* **76**, 3055 (1971).
- ⁶D. P. Sheehan, R. Koslover, and R. McWilliams, *J. Geophys. Res.* **96**, 14107 (1991).
- ⁷M. Bacal and G. W. Hamilton, *Phys. Rev. Lett.* **42**, 1538 (1979).
- ⁸P. A. Bernhardt, *J. Geophys. Res.* **92**, 4617 (1987).
- ⁹R. C. Davidson, *Methods in Nonlinear Plasma Theory* (Academic, New York, 1972).
- ¹⁰G. I. Kent, N. C. Jen, and F. F. Chen, *Phys. Fluids* **12**, 2140 (1969).
- ¹¹M. Porkolab and R. P. H. Chang, *Rev. Mod. Phys.* **50**, 745 (1978).
- ¹²M. V. Goldman, *Rev. Mod. Phys.* **56**, 709 (1984).
- ¹³T. H. Dupree, *Phys. Fluids* **9**, 1773 (1966).
- ¹⁴P. C. Liewer, *Nucl. Fusion* **25**, 543 (1985).
- ¹⁵S. Von Goeler, T. Ohe, and N. D'Angelo, *J. Appl. Phys.* **37**, 2519 (1966).
- ¹⁶H. J. Doucet, *Phys. Lett. A* **33**, 283 (1970).
- ¹⁷A. Y. Wong, D. L. Mamas, and D. Arnush, *Phys. Fluids* **18**, 1489 (1975).
- ¹⁸N. Hershkovitz and T. Intrator, *Rev. Sci. Instrum.* **52**, 1629 (1981).
- ¹⁹T. Intrator, N. Hershkovitz, and R. Stern, *Phys. Fluids* **26**, 1942 (1983).
- ²⁰M. Galvez and P. Gary, *Phys. Fluids* **29**, 4085 (1986).
- ²¹N. D'Angelo and R. L. Merlino, *IEEE Trans. Plasma Phys.* **PP-14**, 285 (1986).
- ²²G. O. Ludwig, J. L. Ferreira, and Y. Nakamura, *Phys. Rev. Lett.* **52**, 275 (1984).
- ²³J. L. Cooney, M. T. Gavin, and K. E. Lonngren, *Phys. Fluids B* **3**, 2758 (1991).
- ²⁴N. D'Angelo, S. von Goeler, and T. Ohe, *Phys. Fluids* **9**, 1605 (1966).
- ²⁵N. Rynn, *Rev. Sci. Instrum.* **35**, 40 (1964).
- ²⁶N. Rynn and N. D'Angelo, *Rev. Sci. Instrum.* **31**, 1325 (1961).
- ²⁷A. Chutjian, *Phys. Rev. Lett.* **46**, 1511 (1981).
- ²⁸D. P. Sheehan and N. Rynn, *Rev. Sci. Instrum.* **59**, 1369 (1988).
- ²⁹D. N. Hill, S. Fornaca, and M. G. Wickham, *Rev. Sci. Instrum.* **54**, 309 (1983).
- ³⁰R. A. Stern, D. N. Hill, and N. Rynn, *Phys. Rev. Lett.* **47**, 792 (1981).
- ³¹T. H. Dupree, *Phys. Fluids* **9**, 1773 (1966).
- ³²T. H. Dupree, *Phys. Fluids* **10**, 1049 (1967).
- ³³R. McWilliams, M. K. Okubo, and N. S. Wolf, *Phys. Fluids B* **2**, 523 (1989).
- ³⁴B. Song, N. D'Angelo, and R. L. Merlino, *Phys. Fluids B* **3**, 284 (1991).
- ³⁵B. Song, R. L. Merlino, and N. D'Angelo, *Phys. Lett. A* **153**, 233 (1991).
- ³⁶R. W. Motley, *Q-Machines* (Academic, New York, 1975).
- ³⁷R. McWilliams and D. P. Sheehan, *Phys. Rev. Lett.* **56**, 2485 (1986).